Evidence of Weak Chaos Within Plug-Slug Transition in Horizontal Two-Phase Flow

1995 Europhys. Lett. 30 75

(http://iopscience.iop.org/0295-5075/30/2/003)

EUROPHYSICS LETTERS 10 April 1995

Europhys. Lett., **30** (2), pp. 75-80 (1995)

Evidence of Weak Chaos within Plug-Slug Transition in Horizontal Two-Phase Flow.

J. DRAHOŠ (*), M. PUNČOCHÁŘ (*), C. SERIO (**) and V. TRAMUTOLI (**)

(*) *Institute of Chemical Process Fundamentals*
Czech Academy of Sciences - Prague, Czech Republic
(**) *Università della Basilicata - Potenza, Italy*

(received 10 November 1994; accepted in final form 17 March 1995)

PACS. 05.45 + b – Theory and models of chaotic systems.
PACS. 02.70 – c – Computational techniques.
PACS. 47.20 – k – Hydrodynamic stability.

Abstract. – Intermittent behaviour has been observed in gas-liquid flows in a horizontal pipe and a weak sign of deterministic chaos has been diagnosed within a transition from plug to slug flow. The analysis has been performed on the basis of an algorithm which exploits the concept of short-term predictability of chaotic motions. The method is completely non-parametric and works whatever the distribution function of the data points may be. The weak sign of chaos is in contrast with the Lorenz-type systems (strong chaos) and supports the idea of Kolmogorov about irregular motion in hydrodynamical systems.

The hydrodynamics of gas-liquid flows has been long studied, but a comprehensive analytical treatment is still lacking because of the inherent computational difficulties involved in the associated Navier-Stokes equation. Information about the dynamics of these systems relies mostly on empirical investigations, typically available in the form of time series of a suitable single observable. As shown in the recent literature [1, 2] a correct definition and identification of flow regimes in gas-liquid flows may be questionable even for stable and seemingly well-developed flow patterns. The difficulties encountered increase substantially in the transition regions where the combination of two or more patterns are present and the resulting character of the flow displays a variety of behaviour depending on the control parameters. This situation occurs also in intermittent-flow patterns in a horizontal pipe, which are usually subdivided into two subregimes: plug flow and slug flow. A plug flow can be found at low gas velocities and consists of small and elongated bubbles flowing at the top of the pipe. The liquid phase is homogeneous and the gas-liquid interface is smooth. Slug flow is a stratified flow with the intermittent appearance of high-velocity liquid slugs which bridge the whole pipe and can be highly aerated. Several criteria have been proposed in the literature for defining the transition between the two regimes: some of them are based on photographic studies, others use the signals from pressure or conductivity probes (*e.g.*, [3]). Needless to say, however, that a satisfactory definition of the plug-slug transition is still lacking. This work has been motivated by observations made in our former measurements [4] where the intermittent flow was studied by using the simultaneous analysis of wall pressure pulsations, static-pressure drop and average velocity of liquid phase. At a given superficial liquid velocity and for increasing gas velocities, the observed character of wall pressure fluctuations changed from a very irregular (caused by the simultaneous presence of many bubbles in the pipe) to a well-patterned periodic signal (typical of the developed slug flow). The corresponding power spectra evolved from a broad-band type towards the spectra with a single dominant peak. However, the amplitude and spectral analysis of pressure fluctuations did not give a reliable discrimination between plug and slug flow in this case. To examine a possible chaotic feature of the plug-slug transition, a new algorithm recently developed by one of the authors ([5-7]) has been used. The algorithm exploits non-linear short-term prediction of a signal as a tool to distinguish between chaos and randomness. The present version of the algorithm does not require any preliminary transform to be applied to the data points in order to provide Gaussian-distributed variables. The method works with time series whose distribution functions may have significant departure from the normal law. Non-linear short-term predictability as a tool to distinguish chaos from randomness dates back to Farmer and Sidorowich [8]. In addition, the topic has been discussed by Sugihara and May [9], Casdagli [10], Kennel and Isabelle [11].

The rationale behind the scheme is that if only a few degrees of freedom interact non-linearly to generate deterministic chaos then a *local* (non-linear) predictor can be constructed which approximates the dynamics of the low-dimensional signal better than any *global* (linear) predictor. Technically, predictors are built by locally and globally fitting autoregressive processes to the data:

$$x(n) = \sum_{j=1}^{p} \varphi_j x(n-j), \qquad (1)$$

where $x(n)$ denote a certain signal, or function of time (we assume that the signal is sampled at equal interval of time, say Δt, then we write $x(t = n\Delta t) = x(n)$; $n = 1, \ldots, N$, N being the number of data points), p is the order of the autoregressive process and φ_j; $j = 1, \ldots, p$, are the autoregression coefficients. These coefficients, in the case of the global (linear) representation do not depend on the time origin n (therefore, they generate a time-shift invariant filter), otherwhise they do.

The *global approach* is equivalent to represent the observations by means of a linear (infinite-dimensional) stochastic model, whereas the *local approach* is equivalent to represent the data on the basis of a low-dimensional deterministic chaotic system. Then, the predictive skill of the two approaches is compared. If the local representation gives a predictive advantage over the global one, and therefore over the entire class of linear stochastic systems including regular attractors and coloured noise, the conclusion is for chaos, otherwise the reverse conclusion is taken.

For both forecasting approaches (local or global), let us define the forecast error for the l-step ahead prediction by: $e(l) = x(n+l) - \hat{x}(n+l)$ (here $\hat{x}(n+l)$ represents the forecast at the time $n+l$), then the normalized root-mean-square forecasting error, $E(l)$, will be defined as the expectation value of the forecast error: $E^2(l) = \langle e^2(l) \rangle / \sigma_x^2$, where the angular brackets denote expectation and σ_x is the standard deviation of the series. $E(l)$ provides a quantitative measure of the predictive skill of each representation (local or global). Provided that the signal $x(t)$ is the output of a chaotic system and $p > D$, where D is the dimension of the underlying attractor, then, subject to very generic assumptions [7, 12], we have that: $E_{\mathrm{gl}}(l) > E_{\mathrm{lc}}(l)$, where E_{gl} denotes the root-mean-square forecasting error affecting the global prediction and $E_{\mathrm{lc}}(l)$ is the corresponding value but in the case of the local prediction.

In applying the above procedure we need a suitable estimation of the optimal order p of the autoregressive model (local or global) fitted to the data points. The rationale for the selection of the optimal order is as follows. We divide the time series into two separate parts: a fitting set $x(1), \ldots, x(N_1)$ and a testing set $x(N_1+1), \ldots, x(N_1+N_2)$, $N = N_1 + N_2$ being the size of the sequence. For each given order p, the first part of the series is used to compute the autoregression coefficients (global or local), then forecasts are produced at the location of the data points in the second part of the series and the corresponding errors, $e_p(l)$ computed. Here, the subscript p remembers that this operation is repeated for different values of p, *i.e.* $p = 1, \ldots, p_u$, where p_u is an upper bound specified from the user. Then, the forecast error function $E_p(l)$ is computed and the norm, $K(p)$, evaluated by $K(p) = \sqrt{E_p^2(1) + \ldots + E_p^2(l_{max})}$. Finally, we adopt as the order of the process, p_{opt}, that p for which $K(p)$ is minimized. Here, l_{max} is the maximum step ahead at which forecasts are obtained. In practice, it is obtained by the condition $E(l_{max}) \approx 1$.

The procedure is used either in the case of the global predictors or in the case of the local ones. In both cases we obtain *true* optimal mean-square predictors. This point is important since for arbitrary p the representation (1) is not necessarily *the best* in the least-square sense. This point is not explicitly recognized, *e.g.*, by Casdagli [10] which uses an approach similar to ours.

Once the optimal predictions have been obtained and the forecast error function $E(l)$ computed, the error bar for $E(l)$ can be estimated by $\mathrm{var}[E^2(l)] \approx E^4(l)(2+\gamma_2)/m$, where γ_2 is the *kurtosis* index of the population $\{e(l)\}$ ($\gamma_2 = 0$ for a Gaussian population) and $m = N_2 - l_{max}$ is the size of the forecast error series.

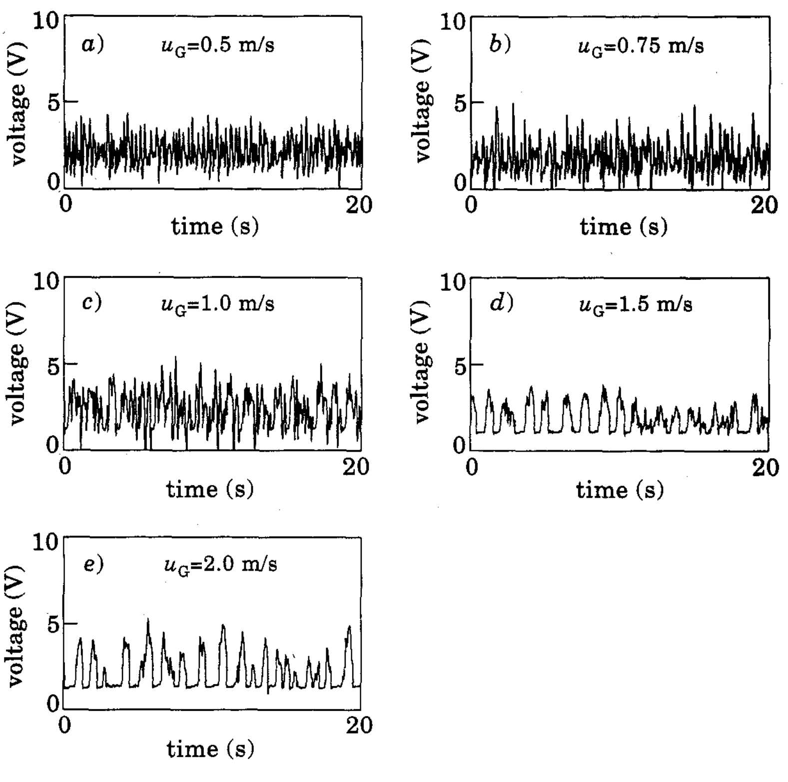

Fig. 1. – The time dependence of the wall pressure fluctuations for the five gas velocities. Only the first 2000 data points of each time series are shown in the figure.

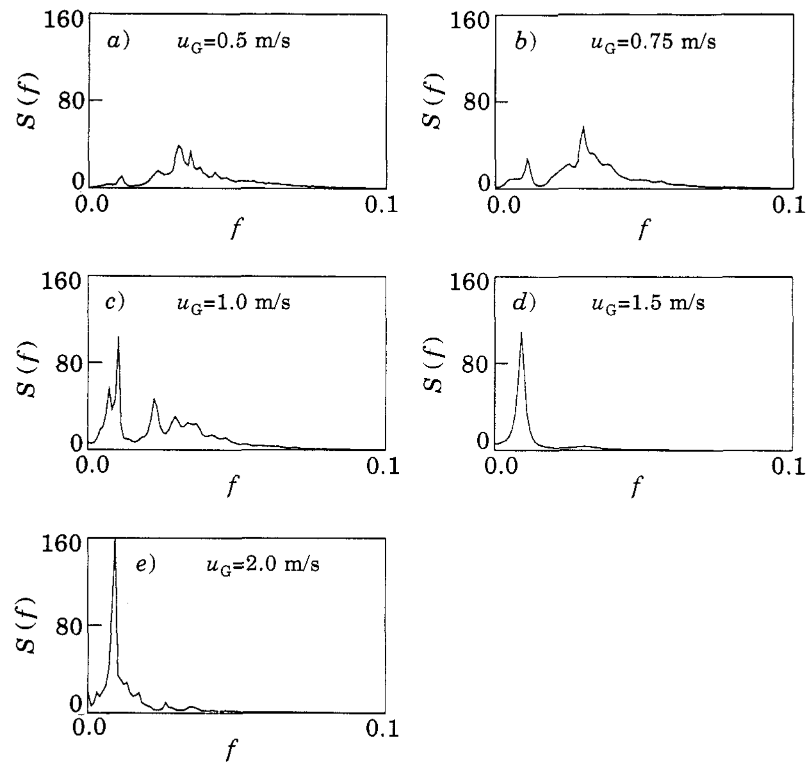

Fig. 2. – Power spectra of the five time series. The frequency scale is normalized to the Nyquist frequency.

The above procedure has been applied to study the character of the transition from plug to slug flow. To this end the wall pressure fluctuations were measured in a horizontal air-water flow. The pipe had an inner diameter of 0.05 m and a total length of 5.1 m. A simple tee mixing configuration was used at the inlet. The detailed description of the experimental loop is given in [13]. The pressure sensor was located 80 diameters downstream from the entrance. According to Nydal *et al.* [14], this distance should be enough to avoid the existence of developing slugs at sufficiently low gas velocities (in our case from 0.1 to 2 m/s). The presence of stable unaerated plugs was confirmed also by high-speed photographs.

The range of superficial velocities was 0.8–1.0 ms^{-1} for liquid and 0.1–2.0 ms^{-1} for the gas phase. Data were sampled at a sampling frequency of 100 Hz using a fast 12-bit A/D converter. The whole observational time was 600 s, therefore the size of each time series is $N = 60\,000$.

For the present work, five time series (see fig. 1) were used corresponding at the five different gas velocities $u_G = 0.5$, 0.75, 1.0, 1.5 and 2.0 ms^{-1}. The superficial liquid velocity was $u_L = 1\ ms^{-1}$ for all the five series. The data at $u_G = 0.5\ ms^{-1}$ are representative also for lower gas velocities so that they will not be considered in the present analysis.

Power spectra are shown for the sequence of the five gas velocities in fig. 2. At $u_G = 0.50\ ms^{-1}$, the signal fluctuates rapidly and the corresponding variance spectrum exhibits a broad-band part together with different sharp features. This corresponds to the simultaneous presence of several elongated bubbles in the pipe. Although the character of the time series for $u_G = 0.75\ ms^{-1}$ is similar, the spectrum seems to be locked in two

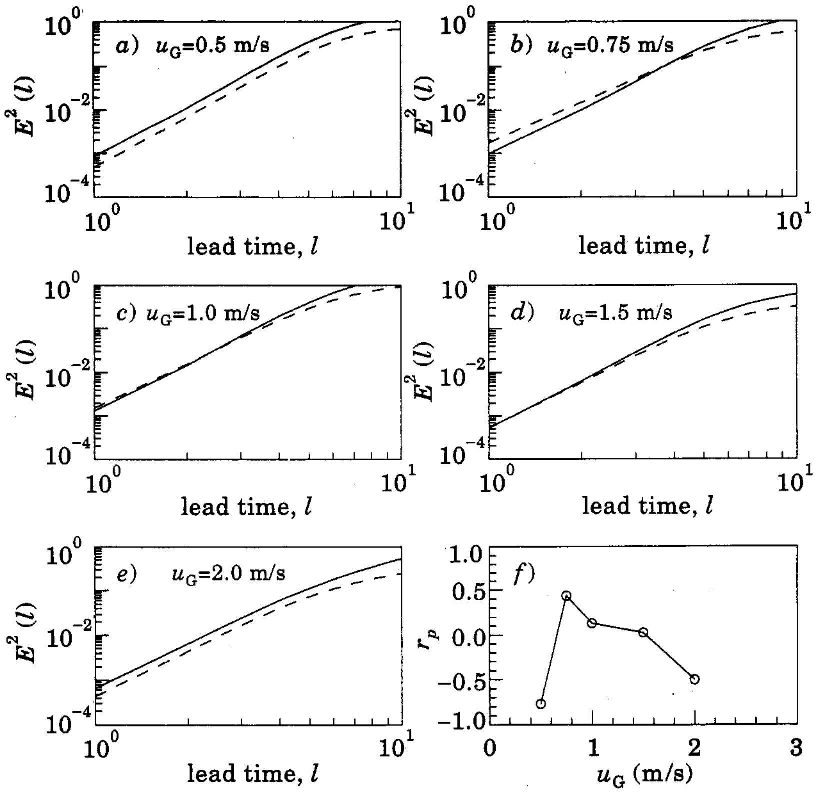

Fig. 3. – Comparison between local (solid line) and global (dashed line) forecast error function, $E^2(l)$, for the five time series. Figure 3*f*) shows a plot of r_p against the gas velocity u_G.

dominant peaks, one at the location $f \approx 0.035$ and the other at lower frequency $f \approx 0.009$. For time series at $u_G = 1.0\ \mathrm{ms}^{-1}$ the baseline begins to appear, which is typical for the slug flow, and its magnitude corresponds roughly to the hydrostatic pressure after passing the slug (*i.e.* if empty space exists between the measuring point and the pipe outlet). The dominant frequency in the lowest part of the spectrum gives the frequency of slugs. For increasing gas velocity this transition continues and become complete at $u_G = 1.5\ \mathrm{ms}^{-1}$ when only one dominant peak emerges in the variance spectrum.

Figure 3 compares for the five series the local and global forecast function, $E^2(l)$. For these computations, according to the methodology discussed above, we divided each time series in a fitting set with $N_1 = 59\,000$ and in a testing series $N_2 = 1000$. Of course, $N_1 + N_2 = N = 60\,000$.

We see from fig. 3 that at $u_G = 0.5\ \mathrm{ms}^{-1}$ the global approach is superior over the local one, but at $u_G = 0.75\ \mathrm{ms}^{-1}$, when the spectrum seems to collapse in two dominant spectral features, the local predictions (up to the 3-step ahead forecast) are superior over the global one. Note that the differences between the two curves are statistically significant up to $l = 2$. The superiority of the global approach over the local one near the zone where $E(l) \approx 1$ is expected since the linear approach is more robust to observational noise than the local one. For $u_G = 1.0\ \mathrm{ms}^{-1}$ the local predictions are still slightly superior but the differences are statistically insignificant. The two curves almost concide for $u_G = 1.5\ \mathrm{ms}^{-1}$ and, finally, separate when $u_G = 2.0\ \mathrm{ms}^{-1}$, that is when the transition to one relevant harmonic has been completed. We see that the frequency coupling visible from the variance spectra is accompanied by a chaotic transition as indicated from the sequence of the five drawings 3*a*)-*e*). The transition from the plug to the slug regime is characterized by an excess of the local predictability over the global one. Thus a proper comparison of the two predictive skills can be used to design an objective index to identify the plug-slug transition. To this end, let us consider the simple index $r_p(u_G) = [E_{gl}^2(1) - E_{lc}^2(1)]/E_{gl}^2(1)$. This index will show a maximum at the value u_G which corresponds to the transition as illustrated in fig. 3*f*).

Finally, from fig. 2 we learn that the spectral density is different from zero only on a limited region of the normalized frequency interval. This does not agree with the idea of strong chaos as modelled in Lorenz-type systems [15]. For these systems a very broad spectrum invades the frequency range. The dynamical consequence, then, is that the trajectories along the attractor are highly sensitive to initial conditions. Our findings support rather the Kolmogorov view of weak chaos in dynamical systems. Kolmogorov-type systems have more relation to the Navier-Stokes equation attractors than those of the Lorenz model (*e.g.*, [16]).

* * *

This work was supported by the Grant Agency of the Czech Republic under No. 104/93/2264 and by Agenzia Spaziale Italiana.

REFERENCES

[1] Mao Z. S. and Dukler A. E., *Int. J. Multiphase Flow*, **19** (1993) 377.
[2] Hewitt G. F. and Jayanti S., *Int. J. Multiphase Flow*, **19** (1993) 527.
[3] Ruder Z. and Hanratty T. J., *Int. J. Multiphase Flow*, **16** (1990) 233.
[4] Drahoš J., Ebner L., Bradka F., Fialova M. and Čermák J., *Proceedings of the International Conference on the Mechanics of Two-Phase Flows* (Nat. Taiwan University, Taipei, ROC) 1989, p. 351.
[5] Serio C., *Nuovo Cimento B*, **107** (1992) 681.
[6] Serio C., *Fractal 93: Fractals in the Natural and Applied Sciences*, edited by M. M. Novak (Elsevier Science B.V., North-Holland) 1994, p. 371.
[7] Serio C., *Europhys. Lett.*, **27** (1994) 103.
[8] Farmer J. D. and Sidorowich J. J., *Phys. Rev. Lett.*, **59** (1987) 845.
[9] Sugihara G. and May R. M., *Nature*, **344** (1990) 734.
[10] Casdagli M., *J. R. Statist. Soc. B*, **54** (1991) 303.
[11] Kennel M. B. and Isabelle S., *Phys. Rev. A*, **6** (1992) 3111.
[12] Cuomo V., Serio C., Crisciani V. and Ferraro A., *Tellus A*, **46** (1994) 299.
[13] Drahoš J., Čermák J., Selucký K. and Ebner L., *Chem. Eng. Process.*, **22** (1987) 45.
[14] Nydal O. J., Pintus S. and Andreussi P., *Int. J. Multiphase Flow*, **18** (1992) 439.
[15] Lorenz E. N., *J. Atmos. Sci.*, **20** (1963) 130.
[16] Arnol'd V., in *Turbulence and Stochastic Processes: Kolmogorov's Idea 50 Years on*, edited by J. C. R. Hunt, O. M. Phillips and D. Williams (The Royal Society, London) 1991.